

Unified treatment of Fermi pockets and arcs scenarios for the cuprates: Sum rule consistent response functions of the pseudogap

Peter Scherpelz,¹ Adam Rançon,¹ Yan He,² and K. Levin¹

¹*James Franck Institute, University of Chicago, Chicago, Illinois 60637, USA*

²*College of Physical Science and Technology, Sichuan University, Chengdu, Sichuan 610064, China*

(Dated: July 3, 2014)

Essential to understanding the cuprate pseudogap phase is a study of the charge (and spin) response functions, which we address here via a consistent approach to the Fermi arcs and the Fermi pockets scenario of Yang, Rice and Zhang (YRZ). The two schemes are demonstrated to be formally similar, and to share a common physics platform; we use this consolidation to address the inclusion of vertex corrections which have been omitted in YRZ applications. We show vertex corrections can be easily implemented in a fashion analytically consistent with sum rules and that they yield important contributions to most observables. A study of the charge ordering susceptibility of the YRZ scenario makes their simple physics evident: they represent the inclusion of charged bosonic, spin singlet degrees of freedom, and are found to lead to a double peak structure.

The discovery of the high temperature superconductors has led to the development of extensions (as well as replacements) for BCS theory in which strong correlations or self energy effects are present simultaneously with the underlying pairing interactions which drive superconductivity. These self energy contributions are associated with the anomalous pseudogap behavior which sets in above T_c and which may persist as well below the transition. A proper treatment of highly correlated normal and superconducting states introduces consistency constraints (vertex corrections, Ward identities and sum rules). This was central in the long history of BCS theory, where these constraints led to an understanding of new types of “particles” or excitations such as the Higgs boson and its related mechanism.

In the high- T_c cuprates, characterizing the spin and charge response has been essential for clarifying whether the pseudogap is associated with pairing or with an alternative ordering, although there is as yet no unanimity.^{1,2} A growing enthusiasm is emerging for one particular pairing-based approach to the pseudogap developed by Yang, Rice and Zhang (YRZ),³ which suggests the possibility of charge ordering in the presence of pairing.⁴ Accompanying this interest has been a fairly universal neglect of vertex corrections^{4,5} in the calculated response functions. This omission is not a formal technicality. At a minimum such corrections are essential in order to ensure that the normal phase is not associated with an unphysical Meissner effect.

This leads to the goal of the present paper, which is to present a calculation of self consistent response functions for the YRZ theory of Fermi pockets³ along with an alternative approach involving Fermi arcs.^{2,6,7} We show here that these two approaches to the pseudogap are in fact closely related, sharing common physical features and allowing nearly identical calculations of vertex corrections. We also show that these vertex corrections are consistent with sum rule constraints. Finally, we demonstrate that introducing self consistency leads to (hitherto ignored^{4,5}) contributions to the spin and charge response, which are

of sizable magnitude and can be physically understood.

The consolidation that we present between Fermi arcs and pockets is possible because both theories contain pairs which are present in the pseudogap phase. These pairs, with their bosonic character, lead to similar vertex corrections in both theories. Formally, these pseudogap pairs arise from the semi-microscopic self energies posited by the theories,^{2,3} which contain both superconducting (sc) and pseudogap (pg) components: $\Sigma = \Sigma_{sc} + \Sigma_{pg}$. The form of Σ_{pg} is rather similar to the BCS-like self energy of the condensate but in the pockets case this term leads to a reconstructed Fermi surface (“pockets”) and in the arcs case to a blurring of the d -wave nodes (“arcs”). This two-gap form of Σ ensures that the pseudogap correlations persist below T_c , but are distinct from condensation. It should not be confused with (one-gap) phase fluctuation models, where it is presumed that the pseudogap turns into a condensate gap at the transition. We show here how to impose consistency for both two-gap approaches by addressing the f-sum rule on the charge density response (above T_c) and the transverse sum rule on the current density response at all T . In this way vertex corrections emerge naturally and can be readily incorporated into the Fermi pockets approach of YRZ. (They have been included in the formally related Fermi arcs approach in Refs. 6 and 8.)

For the pockets model of YRZ the microscopic picture for the pg contribution is that it is associated with resonating pairs of spin singlets^{9,10} which, when holes are injected, become charged. In the Fermi arcs model, where we consider a two-gap rendition,² (which introduces both sc and pg gaps Δ_{sc} and Δ_{pg} , as in YRZ), the pg correlations represent finite momentum, out of the condensate excitations; they reflect a stronger-than-BCS attractive interaction. This scenario for a pseudogap is realized in the laboratory of ultracold Fermi gases² and associated with BCS-BEC crossover. The excited pairs are *gradually* converted to condensed pairs as the temperature is lowered below T_c . Here Δ_{pg}^2 is effectively zero at temperature $T = 0$ and reaches a max-

imum at T_c ; in this way the square of the excitation gap $\Delta^2 = \Delta_{sc}^2 + \Delta_{pg}^2$ is relatively constant below T_c . Just as in the YRZ pockets model, this Fermi arcs model has addressed thermodynamics⁷, Nernst¹¹, the penetration depth^{6,12}, quasiparticle interference in STM^{13,14} as well as the ac and dc conductivities^{15–17} and diamagnetism.¹⁸ Perhaps its greatest success is that it naturally leads to a nodal-antinodal dichotomy.¹⁹ This refers to the collapse of the arcs as temperature approaches T_c from above; as T approaches T_c from below the nodal ARPES gap has a T dependence which reflects that of the order parameter, Δ_{sc} , while the antinodal gap is very little affected by the transition.

Theory and response functions. We introduce the Green's function (and neglect for simplicity the incoherent contributions)

$$G_K = \frac{1}{\omega - \xi_{\mathbf{k}} - \frac{\Delta_{pg}^2}{\omega + \xi_{\mathbf{k}}^{pg}} - \frac{\Delta_{sc}^2}{\omega + \xi_{\mathbf{k}} + \Sigma_R(\mathbf{k}, -\omega)}}, \quad (1)$$

where $K = (\omega, \mathbf{k})$. Here for the arcs and pockets models respectively

$$\begin{aligned} \xi_{\mathbf{k}}^{pg} &= \xi_{\mathbf{k}} + i\gamma \quad \text{and} \quad \Sigma_R(\mathbf{k}, \omega) \equiv 0, \\ \xi_{\mathbf{k}}^{pg} &= \xi_{\mathbf{k}}^0 \quad \text{and} \quad \Sigma_R(\mathbf{k}, \omega) = \frac{\Delta_{pg}^2}{\omega + \xi_{\mathbf{k}}^{pg}}, \end{aligned} \quad (2)$$

where the dispersion $\xi_{\mathbf{k}}^{(0)}$ is introduced in Ref. 3. There are two different assumed forms²⁰ for the sc piece in the YRZ approach, and here we take the original one,³ rather than introduce corrections associated with phenomenological adjustments. Similarly we stress that for the arcs model we can minimize phenomenological input and simply take the central free parameter γ as independent of temperature. The role of γ , which has a microscopic basis,²¹ is critical; it leads to a smearing of the d -wave node and thus to the Fermi arcs.^{19,22–24}

The pseudogap and superconducting self energy in both schemes are given by

$$\begin{aligned} \Sigma_{pg}(K) &= -\Delta_{pg}^2 G_0^{pg}(-K) = -\Delta_{pg}^2 \times \frac{1}{\omega + \xi_{\mathbf{k}}^{pg}}, \\ \Sigma_{sc}(K) &= -\Delta_{sc}^2 G_0^{sc}(-K) = -\Delta_{sc}^2 \times \frac{1}{\omega + \xi_{\mathbf{k}} + \Sigma_R(\mathbf{k}, -\omega)} \end{aligned}$$

which defines G_0^{pg} and G_0^{sc} . Because $\xi_{\mathbf{k}}^{pg} \neq \xi_{\mathbf{k}}$, the YRZ scheme arrives at a many-body reconstructed bandstructure. Moreover, we see from G in both the arcs and pockets models that the form of Σ_{pg} is not very different from

that of Σ_{sc} , yet their effects on the physics of the generalized response functions have to be profoundly different. We enforce this difference by ensuring that there can be no Meissner effect in the normal phase, and this requires the inclusion of vertex corrections in the current-current response function which we write as \vec{P} . It will be convenient to introduce a parameter $\Lambda^{sc} \equiv 1$ for the pockets case and $\Lambda^{sc} \equiv 0$ for the arcs scenario. We also define

$$\begin{aligned} F_{pg,K} &\equiv -\Delta_{pg} G_0^{pg}(-K) G_K, \\ F_{sc,K} &\equiv -\Delta_{sc} G_0^{sc}(-K) G_K. \end{aligned} \quad (3)$$

The quantity F_{pg} (unlike F_{sc}) is *not* to be associated with superfluidity. It is not in the notation “ F ” that superfluidity enters, it is in the way in which the current-current correlator is constructed, as we show below.

Next, we obtain an expression for the diamagnetic current contribution $(\frac{n}{m})_{dia} \equiv 2 \sum_K \frac{\partial^2 \xi_{\mathbf{k}}}{\partial \mathbf{k} \partial \mathbf{k}} G(K)$. For notational simplicity we drop terms which involve the k derivative of the d -wave form factor throughout. These effects can be readily inserted, but are seen to be negligible in magnitude. We find that the diamagnetic current can be rewritten via integration by parts, using $\partial G(K)/\partial \mathbf{k} = -G^2(K) \partial G^{-1}(K)/\partial \mathbf{k}$ so that $(\frac{n}{m})_{dia}$

$$\begin{aligned} &= -2 \sum_K G_K^2 \frac{\partial \xi_{\mathbf{k}}}{\partial \mathbf{k}} \frac{\partial \xi_{\mathbf{k}}}{\partial \mathbf{k}} + 2 \sum_K F_{pg,K}^2 \frac{\partial \xi_{\mathbf{k}}^{pg}}{\partial \mathbf{k}} \frac{\partial \xi_{\mathbf{k}}}{\partial \mathbf{k}} \\ &+ 2 \sum_K F_{sc,K}^2 \left[\frac{\partial \xi_{\mathbf{k}}}{\partial \mathbf{k}} \frac{\partial \xi_{\mathbf{k}}}{\partial \mathbf{k}} - \Lambda^{sc} \frac{\partial \xi_{\mathbf{k}}^{pg}}{\partial \mathbf{k}} \frac{\partial \xi_{\mathbf{k}}}{\partial \mathbf{k}} \Delta_{pg}^2 (G_0^{pg}(K))^2 \right]. \end{aligned} \quad (4)$$

Given the parameterized self energies introduced above, *in this exact expression, central to this paper, the second term on each line provides a template for the form of the ignored vertex corrections in the response functions.* That there is no Meissner effect above T_c implies that the current-current correlation function at zero wavevector and frequency, $\vec{P}(0) = -(\frac{n}{m})_{dia}$. Below T_c in the YRZ scheme we make use of the superconducting Ward identity²⁵ (see Supplemental Materials) to establish that the prefactor of F_{sc}^2 of Eq. (4) enters into $-\vec{P}(0)$ with the opposite sign compared to the diamagnetic current. Once we know the form for $\vec{P}(0)$ we can make an ansatz for the form of $\vec{P}(Q)$ (compatible with BCS theory when $\Delta_{pg} \equiv 0$). While there is no unique inference for $\vec{P}(Q)$ away from $Q = 0$, we depend on the explicit satisfaction of the transverse and f-sum rules to support our ansatz. Our precise form for $\vec{P}(0)$ and our ansatz for $\vec{P}(Q)$ are given by

$$-\vec{P}(0) = -2 \sum_K G_K^2 \frac{\partial \xi_{\mathbf{k}}}{\partial \mathbf{k}} \frac{\partial \xi_{\mathbf{k}}}{\partial \mathbf{k}} + 2 \sum_K F_{pg,K}^2 \frac{\partial \xi_{\mathbf{k}}^{pg}}{\partial \mathbf{k}} \frac{\partial \xi_{\mathbf{k}}}{\partial \mathbf{k}} - 2 \sum_K F_{sc,K}^2 \left[\frac{\partial \xi_{\mathbf{k}}}{\partial \mathbf{k}} \frac{\partial \xi_{\mathbf{k}}}{\partial \mathbf{k}} - \Lambda^{sc} \frac{\partial \xi_{\mathbf{k}}^{pg}}{\partial \mathbf{k}} \frac{\partial \xi_{\mathbf{k}}}{\partial \mathbf{k}} \Delta_{pg}^2 (G_0^{pg}(K))^2 \right], \quad (5)$$

$$\vec{P}(Q) = 2 \sum_K \frac{\partial \xi_{\mathbf{k}+\mathbf{q}/2}}{\partial \mathbf{k}} \frac{\partial \xi_{\mathbf{k}+\mathbf{q}/2}}{\partial \mathbf{k}} G_K G_{K+Q} - 2 \sum_K \frac{\partial \xi_{\mathbf{k}+\mathbf{q}/2}^{pg}}{\partial \mathbf{k}} \frac{\partial \xi_{\mathbf{k}+\mathbf{q}/2}}{\partial \mathbf{k}} F_{pg,K} F_{pg,K+Q}$$

$$+ 2 \sum_K F_{\text{sc},K} F_{\text{sc},K+Q} \left[\frac{\partial \xi_{\mathbf{k}+\mathbf{q}/2}}{\partial \mathbf{k}} \frac{\partial \xi_{\mathbf{k}+\mathbf{q}/2}}{\partial \mathbf{k}} - \Lambda^{\text{sc}} \frac{\partial \xi_{\mathbf{k}+\mathbf{q}/2}^{\text{pg}}}{\partial \mathbf{k}} \frac{\partial \xi_{\mathbf{k}+\mathbf{q}/2}}{\partial \mathbf{k}} \Delta_{\text{pg}}^2 G_0^{\text{pg}}(K) G_0^{\text{pg}}(K+Q) \right], \quad (6)$$

where we only consider the transverse response P_t below T_c (the longitudinal part of $\vec{P}(Q)$ is correct in the normal phase, but requires collective mode corrections for $T < T_c$).

The quantities $\vec{P}(0)$ and $(\frac{\vec{n}}{m})_{\text{dia}}$, are, however, all that is needed to deduce an expression for the superfluid density $\frac{n_s}{m} \equiv (\frac{n}{m})_{\text{dia}} - P_t(0)$ in both the arcs and pockets model,

$$\frac{n_s}{m} = 4 \sum_K F_{\text{sc},K}^2 \left[\frac{\partial \xi_{\mathbf{k}}}{\partial \mathbf{k}} \frac{\partial \xi_{\mathbf{k}}}{\partial \mathbf{k}} - \Lambda^{\text{sc}} \frac{\partial \xi_{\mathbf{k}}^{\text{pg}}}{\partial \mathbf{k}} \frac{\partial \xi_{\mathbf{k}}}{\partial \mathbf{k}} \Delta_{\text{pg}}^2 (G_0^{\text{pg}}(K))^2 \right]. \quad (7)$$

It is interesting to note that in the review on YRZ²⁰, a concern was raised that the penetration depth (or n_s/m) which appears in the YRZ literature is missing a vertex correction. Here, with Eqs. (4)-(5), we have established the form for such a vertex correction.²⁶

In the normal state and for both the pockets and arcs model, one can show that the density-density response function is given by

$$P_{\rho\rho}(Q) = 2 \sum_K \left([G_K G_{K+Q}] + [F_{\text{pg},K} F_{\text{pg},K+Q}] \right). \quad (8)$$

This equation will be used in the remainder of this paper to establish the way in which previously omitted⁴ vertex corrections in the second term impact the charge response functions. We restrict calculations to $T > T_c$ so as to avoid complications from collective modes in the presence of pseudogap effects. We can similarly address the quasi-particle interference pattern^{13,14} of STM, as well as the complex conductivity and diamagnetic susceptibility,¹⁵⁻¹⁸ all of which are given in the Supplementary Materials.

Finally, the spin current and density response functions can be similarly deduced. Indeed $(\frac{\vec{n}}{m})_{\text{dia}}$ in Eq. (4), appears in the constraining sum rules on the vertex corrections. The spin-current correlation function is given by $\vec{P}(Q)$ with a sign change in front of F_{sc} , reflecting the absence of a Meissner effect, as the spin pairing is assumed to be singlet. Above T_c , the bare dynamic susceptibility $\chi^{\text{spin}}(Q)$ is the same as the expression in Eq. (8), where the second term represents the vertex corrections. These are necessary to ensure that the formation of singlets leads to a normal state gap in the spin excitation spectrum, which is not fully accounted for by the first term. Below T_c , $\chi^{\text{spin}}(Q)$ must include the vertex corrections associated with Λ^{sc} , but there are no collective mode effects.

Consistency with sum rules. The normal state f-sum rule (on a lattice) provides a strong constraint on the

charge susceptibility in Eq. (8) of the form:

$$\int \frac{d\omega}{\pi} (-\omega \text{Im} P_{\rho\rho}(Q)) = 2 \sum_{\mathbf{k}} (\xi_{\mathbf{k}+\mathbf{q}} + \xi_{\mathbf{k}-\mathbf{q}} - 2\xi_{\mathbf{k}}) n_{\mathbf{k}}, \quad (9)$$

with $n_{\mathbf{k}} = \langle \hat{c}_{\mathbf{k},\sigma}^\dagger \hat{c}_{\mathbf{k},\sigma} \rangle$ (here $Q = (\omega + i0^+, \mathbf{q})$). In the YRZ pockets model, the left-hand side of Eq. (9) gives

$$\begin{aligned} \int \frac{d\omega}{\pi} (-\omega \text{Im} P_{\rho\rho}(Q)) &= 2 \sum_{\mathbf{k}, \alpha=\pm, i=1,2} (-1)^{i-1} f(E_{i,\alpha}) \\ &\times \frac{(E_{i,\alpha} + \xi_{\alpha}^{\text{pg}})(E_{i,\bar{\alpha}} + E_{i,\bar{\alpha}} + \xi_{\bar{\alpha}}^{\text{pg}} - E_{i,\alpha}) + \Delta_{\text{pg}}^2}{E_{1,\alpha} - E_{2,\alpha}}, \end{aligned} \quad (10)$$

where $E_{i,\mathbf{k}} = \frac{1}{2} (\xi_{\mathbf{k}} - \xi_{\mathbf{k}}^{\text{pg}} + (-1)^{i-1} \sqrt{(\xi_{\mathbf{k}} + \xi_{\mathbf{k}}^{\text{pg}})^2 + 4\Delta_{\text{pg}}^2})$, $i = 1, 2$ are the poles of the YRZ Green's function, and we define $\alpha = \pm$ to represent $\mathbf{k} \pm \mathbf{q}/2$. We introduce $\bar{\alpha} = -\alpha$ and $\bar{1} = 2$, $\bar{2} = 1$. Using the two identities $E_{i,\bar{\alpha}} + E_{i,\bar{\alpha}} + \xi_{\bar{\alpha}}^{\text{pg}} = \xi_{\bar{\alpha}}$, and $E_{i,\alpha}(E_{i,\alpha} + \xi_{\alpha}^{\text{pg}}) = \xi_{\alpha}(E_{i,\alpha} + \xi_{\alpha}^{\text{pg}}) + \Delta_{\text{pg}}^2$, as well as the change of variable $\mathbf{k} \rightarrow \mathbf{k} - \alpha\mathbf{q}/2$, we find the right-hand side of Eq. (10) reads

$$\begin{aligned} 2 \sum_{\mathbf{k}, i=1,2} (-1)^{i-1} f(E_{i,\mathbf{k}}) \frac{(E_{i,\mathbf{k}} + \xi_{\mathbf{k}}^{\text{pg}})(\xi_{\mathbf{k}+\mathbf{q}} + \xi_{\mathbf{k}-\mathbf{q}} - 2\xi_{\mathbf{k}})}{E_{1,\mathbf{k}} - E_{2,\mathbf{k}}} \\ = 2 \sum_{\mathbf{k}} (\xi_{\mathbf{k}+\mathbf{q}} + \xi_{\mathbf{k}-\mathbf{q}} - 2\xi_{\mathbf{k}}) n_{\mathbf{k}}, \end{aligned}$$

which is the longitudinal f-sum rule for YRZ in the normal state, since

$$n_{\mathbf{k}} = \frac{(E_{1,\mathbf{k}} + \xi_{\mathbf{k}}^{\text{pg}})f(E_{1,\mathbf{k}}) - (E_{2,\mathbf{k}} + \xi_{\mathbf{k}}^{\text{pg}})f(E_{2,\mathbf{k}})}{E_{1,\mathbf{k}} - E_{2,\mathbf{k}}}.$$

The derivation in the arc case is essentially the same, with $\xi_{\mathbf{k}}^{\text{pg}} = \xi_{\mathbf{k}}$ and $E_{\mathbf{k},2} = -E_{\mathbf{k},1}$.

It should also be clear that the f-sum rule in Eq. (9) assumes a more subtle form in the presence of a lattice, as it does not directly depend on $(\frac{n}{m})_{\text{dia}} \times q^2$. One should think of $(\frac{n}{m})_{\text{dia}}$ as reflecting a $q \rightarrow 0$ limit of the response functions, whereas the f-sum rule was proved above to be valid for all q .²⁷ Finally, the transverse sum rule is shown in the Supplementary Materials to be consistent with Eq. (6).

Numerical results and discussion. We turn now to a quantification of vertex corrections and show that this leads to a much better understanding of their physical nature and origin. Results using the method of calculation presented in Ref. 4 arising from only including the so-called ‘‘bubble’’ contribution are shown as dotted lines

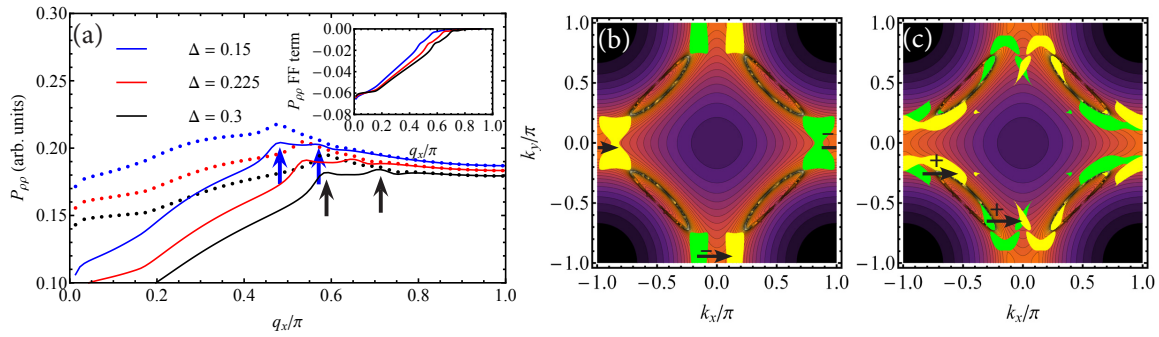


Figure 1. (a) Normal state $\omega = 0$, $q_y = 0$ charge susceptibility $P_{\rho\rho}$ with (solid) and without (dotted) vertex corrections. The arrows indicate that a second peak is present in the former case. Here we follow the band structure used in Ref. 4, and use $T = 0.01$ and broadening $\eta = 0.01^4$ to study a low-temperature system. The doping $p = 0.12$, and chemical potential μ is fixed by the Luttinger sum rule³. These values are normalized to t , the primary single-particle dispersion parameter^{3,4}. The inset shows the contribution of the vertex term ($F_{\text{pg}} F_{\text{pg}}$) to $P_{\rho\rho}$. (b-c) Plots of the momentum phase space contributions to $P_{\rho\rho}(\omega = 0, \mathbf{q} = (0.3\pi, 0))$ for $\Delta = 0.15$, overlaid on contour plots of the spectral function $A_{\text{YRZ}}(\omega = 0, \mathbf{k})$. Shown are green \mathbf{k} (“origin”) regions and yellow $\mathbf{k} + \mathbf{q}$ (“destination”) regions for which the integrand magnitude is greater than a set threshold. (b) shows contributions from the vertex term greater than a threshold of 0.008, while (c) shows single fermionic bubble (GG) contributions greater than a threshold of 0.02. The plus and minus signs in (b) and (c) indicate the sign of the phase space contribution.

in the left panel of Figure 1 with a single peak. They are compared with the full charge susceptibility in Eq. (8), shown as solid lines. As the gap Δ_{pg} increases, the magnitude of the (negative) vertex correction term tends to increase, as indicated in the inset. Importantly, the arrows indicate that this introduces a second peak which is of equal magnitude for larger Δ_{pg} . In the small \mathbf{q} regime vertex corrections remove almost half the weight found in the dotted line bubble contribution.

To understand the physical cause of these vertex corrections, we plot in the middle panel a color contour figure of the dominant phase space contributions to the integrand in Eq. (8) deriving from the vertex corrections for a fixed \mathbf{q} , as indicated by the arrows. These corrections are rather strongly localized to the antinodes. To elucidate this we note that F_{pg} given in Eq. (3) can be interpreted as a bosonic Green’s function since its spectral function exhibits the appropriate sign change when $\omega \rightarrow -\omega$. This bosonic degree of freedom is naturally associated with fermionic pairing and is expected, then, to reside near the antinodes and to increase in magnitude as pairing gets stronger. We may then interpret the vertex corrections in Eq. (8) as arising from the spin singlets in a resonating valence bond (RVB)^{9,10} context, leading to a picture which is not so different from that expounded in Ref. 28. By contrast, the right hand panel indicates the phase space contributions arising from the simple GG “bubble” which tend not to be so relatively strong near the antinode.

Conclusions. All of the results presented here follow rather directly from the form of the self energy Σ_{pg} which,

through a Ward identity, will affect correlation functions in a way which we have just interpreted. An emerging theme is that even though there has been no explicit reference to the spin singlets of RVB, these arguments indicate that one has a two-constituent system. Ignoring vertex corrections in the case of the charge susceptibility is largely ignoring this bosonic constituent. Indeed, even in thermodynamics, not just in the spin and charge response functions, one should expect some residue of bosonic degrees of freedom both directly and indirectly through the gap which they present to the fermionic sector.

Analogous studies are presented for the arcs scenario, except that there are no “hot spots” or pocket tips to lead to sharp peaks in the charge susceptibility.²⁹ This is illustrated in the Supplementary Materials. But more significant is the similarity which allows a consolidation of two (at first sight) rather different approaches to the cuprate pseudogap: the pockets model of YRZ^{3,9} and the arcs model of BCS-BEC crossover.² Both of these have two distinct gaps corresponding to the condensed and non-condensed pairs, although the YRZ is more specific by associating singlet pairing with antiferromagnetic correlations. As noted in Ref. 3, throughout the temperature range, “both gaps keep their own identity”. For this reason, among others, these two-gap approaches are distinguished from phase fluctuation scenarios,³⁰ and allow the general and consistent treatment of response functions presented here.

This work is supported by NSF-MRSEC Grant 0820054.

¹ P. A. Lee, N. Nagaosa, and X. G. Wen, Rev. Mod. Phys. **78**, 17 (2006).

² Q. J. Chen, J. Stajic, S. N. Tan, and K. Levin, Phys. Rep.

- 412**, 1 (2005).
- ³ K.-Y. Yang, T. M. Rice, and F.-C. Zhang, Phys. Rev. B **73**, 174501 (2006).
 - ⁴ R. Comin, A. Frano, M. M. Yee, Y. Yoshida, H. Eisaki, E. Schierle, E. Weschke, R. Sutarto, F. He, A. Soumyanarayanan, Y. He, M. L. Tacon, I. S. Elfimov, J. E. Hoffman, G. A. Sawatzky, B. Keimer, and A. Damascelli, Science **343**, 390 (2014).
 - ⁵ J. P. Carbotte and K. A. G. Fisher and J. P. F. LeBlanc and E. J. Nicol, Phys. Rev. B **81**, 014522 (2010); Phillip E. C. Ashby and J. P. Carbotte, Phys. Rev. B **87**, 184514 (2013); B. Valenzuela and E. Bascones, Phys. Rev. Lett. **98**, 227002 (2007); E. Bascones and B. Valenzuela, Phys. Rev. B **77**, 024527 (2008); A. Pound, J. Carbotte and E. Nicol, Eur. Phys. Journal B–Condensed Matter, **81**, 69 (2011).
 - ⁶ Q. J. Chen, I. Kosztin, B. Jankó, and K. Levin, Phys. Rev. Lett. **81**, 4708 (1998).
 - ⁷ Q. J. Chen, K. Levin, and I. Kosztin, Phys. Rev. B **63**, 184519 (2001).
 - ⁸ I. Kosztin, Q. J. Chen, Y.-J. Kao, and K. Levin, Phys. Rev. B **61**, 11662 (2000).
 - ⁹ P. W. Anderson, P. A. Lee, M. Randeria, T. M. Rice, N. Trivedi, and F. C. Zhang, J. Phys. - Condens. Matter. **16**, R755 ((2004)).
 - ¹⁰ P. W. Anderson, *The Theory of Superconductivity in the High- T_c Cuprate Superconductors* (Princeton University Press, Princeton, 1997).
 - ¹¹ S. Tan and K. Levin, Phys. Rev. B **69**, 064510 (2004).
 - ¹² J. Stajic, A. Iyengar, K. Levin, B. R. Boyce, and T. R. Lemberger, Phys. Rev. B **68**, 024520 (2003).
 - ¹³ D. Wulin, Y. He, C.-C. Chien, D. K. Morr, and K. Levin, Phys. Rev. B **80**, 134504 (2009).
 - ¹⁴ D. Wulin, C.-C. Chien, D. K. Morr, and K. Levin, Phys. Rev. B **81**, 100504R (2010).
 - ¹⁵ D. Wulin, H. Guo, C.-C. Chien, and K. Levin, Phys. Rev. B **86**, 134518 (2012).
 - ¹⁶ D. Wulin and K. Levin, Phys. Rev. B **86**, 134519 (2012).
 - ¹⁷ D. Wulin, B. M. Fregoso, H. Guo, C.-C. Chien, and K. Levin, Phys. Rev. B **84**, 140509(R) (2011).
 - ¹⁸ D. Wulin and K. Levin, Phys. Rev. B **86**, 184513 (2012).
 - ¹⁹ C.-C. Chien, Y. He, Q. Chen, and K. Levin, Phys. Rev. B **79**, 214527 (2009).
 - ²⁰ T. M. Rice, K.-Y. Yang, and F. C. Zhang, Rep. Prog. Phys. **75**, 016502 (2012).
 - ²¹ B. Jankó, J. Maly, and K. Levin, Phys. Rev. B **56**, R11407, (1997); J. Maly, B. Jankó, and K. Levin, Physica C **321**, 113 (1999) and cond-mat/9710187.
 - ²² M. R. Norman, A. Kanigel, M. Randeria, U. Chatterjee, and J. C. Campuzano, Phys. Rev. B **76**, 174501 (2007).
 - ²³ Q. J. Chen and K. Levin, Phys. Rev. B **78**, 020513(R) (2008).
 - ²⁴ A. V. Chubukov, M. R. Norman, A. J. Millis, and E. Abrahams, Phys. Rev. B **76**, 180501(R) (2007).
 - ²⁵ J. R. Schrieffer, *Theory of Superconductivity*, 1st ed. (W.A. Benjamin, Inc., 1964).
 - ²⁶ It should be noted that this vertex correction (which, for the pockets scenario, depends on the cross term $\Delta_{sc}^2 \Delta_{pg}^2$) introduces an effective gap shape which differs from the simple d -wave form.
 - ²⁷ Despite this rather strong validation of the generalized response functions, we note that for both the arcs and pockets models one will not satisfy the compressibility sum rule. This can be traced to the assumed, simplified form for the self energies which are not functions of $\omega + \mu$ as they would be expected to be from the gauge invariance of the microscopic Hamiltonian.
 - ²⁸ V. B. Geshkenbein, L. B. Ioffe, and A. I. Larkin, Phys. Rev. B **55**, 3173 (1997).
 - ²⁹ Y. He, P. Scherpelz, and K. Levin, Phys. Rev. B **88**, 064516 (2013).
 - ³⁰ A. J. James, R. M. Konik, K. Huang, W. Q. Chen, T. M. Rice, and F. C. Zhang, Jour. of Physics: Conference Series **449**, 012006 (2013).

Supplemental materials

VERTEX CORRECTIONS IN CONDUCTIVITY, DIAMAGNETISM AND QUASI-PARTICLE INTERFERENCE

Once one has the current-current response function with vertex corrections

$$\begin{aligned} \vec{P}(Q) = & 2 \sum_K \frac{\partial \xi_{\mathbf{k}+\mathbf{q}/2}}{\partial \mathbf{k}} \frac{\partial \xi_{\mathbf{k}+\mathbf{q}/2}}{\partial \mathbf{k}} G_K G_{K+Q} - 2 \sum_K \frac{\partial \xi_{\mathbf{k}+\mathbf{q}/2}^{\text{pg}}}{\partial \mathbf{k}} \frac{\partial \xi_{\mathbf{k}+\mathbf{q}/2}}{\partial \mathbf{k}} F_{\text{pg},K} F_{\text{pg},K+Q} \\ & + 2 \sum_K F_{\text{sc},K} F_{\text{sc},K+Q} \left[\frac{\partial \xi_{\mathbf{k}+\mathbf{q}/2}}{\partial \mathbf{k}} \frac{\partial \xi_{\mathbf{k}+\mathbf{q}/2}}{\partial \mathbf{k}} - \Lambda^{\text{sc}} \frac{\partial \xi_{\mathbf{k}+\mathbf{q}/2}^{\text{pg}}}{\partial \mathbf{k}} \frac{\partial \xi_{\mathbf{k}+\mathbf{q}/2}}{\partial \mathbf{k}} \Delta_{\text{pg}}^2 G_0^{\text{pg}}(K) G_0^{\text{pg}}(K+Q) \right], \end{aligned} \quad (1)$$

the complex conductivity and diamagnetic susceptibility are given by

$$\sigma_{xx}(\omega) = -\lim_{\mathbf{q} \rightarrow 0} \frac{P_{xx}(\mathbf{q}, \omega) + (n/m)_{xx}^{\text{dia}}}{i\omega} \quad \chi^{\text{dia}} = -\lim_{q_y \rightarrow 0} \text{Re} \left[\frac{P_{xx}(\mathbf{q}, \omega = 0) + (n/m)_{xx}^{\text{dia}}}{\mathbf{q}^2} \right]_{q_x=q_z=0}. \quad (2)$$

The quasi-particle interference pattern reflects the Fourier transform of the changes in the local density of states (LDOS) due to the presence of impurities, which are characterized by a potential U_0 . Here, too, because of the pg self-energy, vertex contributions enter. The LDOS with vertex corrections is given by

$$\delta n(\omega, \mathbf{q}) \propto \text{Im} \int \frac{d^2 k}{(2\pi)^2} \left(G_K G_{K+Q_0} - F_K^{\text{sc}} F_{K+Q_0}^{\text{sc}} \times [1 - \Lambda^{\text{sc}} G_0^{\text{pg}}(K) G_0^{\text{pg}}(K+Q_0) \Delta_{\text{pg}}^2] - F_K^{\text{pg}} F_{K+Q_0}^{\text{pg}} \right),$$

with $Q_0 \equiv (0, \mathbf{q})$ and $K = (\omega, \mathbf{k})$.

WARD IDENTITIES AND VERTEX FUNCTIONS

Normal Pseudogap phase

The Ward identity for the full vertex function $\Gamma_\mu(K, Q) = (\Gamma_0(K, Q), \mathbf{\Gamma}(K, Q))$ in the normal phase is given by

$$\begin{aligned} -\Omega \Gamma_0(K, Q) - i \text{div}_{\mathbf{q}} \mathbf{\Gamma}(K, Q) &= G_K^{-1} - G_{K+Q}^{-1}, \\ &= -\Omega + \xi_{\mathbf{k}+\mathbf{q}} - \xi_{\mathbf{k}} + \Delta_{\text{pg}}^2 \left(\frac{1}{\omega + \Omega + \xi_{\mathbf{k}+\mathbf{q}}^{\text{pg}}} - \frac{1}{\omega + \xi_{\mathbf{k}}^{\text{pg}}} \right), \end{aligned} \quad (3)$$

where $Q = (\Omega, \mathbf{q})$, $K = (\omega, \mathbf{k})$, and $\text{div}_{\mathbf{q}} \mathbf{\Gamma}(K, Q)$ represent the Fourier transform of the divergence of $\mathbf{\Gamma}$, generalized to the lattice. (Note that $\text{div}_{\mathbf{q}} \mathbf{\Gamma}(K, Q) \neq i \mathbf{q} \mathbf{\Gamma}(K, Q)$ for lattice models, unless $q \rightarrow 0$.) The first line of Eq (3) is exact due to charge conservation, whereas the second line follows from the choice of the self-energy (see main text). For the bare vertex function $\gamma_\mu(K, Q) = (\gamma_0(K, Q), \boldsymbol{\gamma}(K, Q))$, this corresponds to

$$\begin{aligned} \gamma_0(K, Q) &= 1, \\ -i \text{div}_{\mathbf{q}} \boldsymbol{\gamma}(K, Q) &= \xi_{\mathbf{k}+\mathbf{q}} - \xi_{\mathbf{k}}. \end{aligned} \quad (4)$$

From Eq. (3), we can infer that the vertex function is given by

$$\begin{aligned} \Gamma_0(K, Q) &= \gamma_0(K, Q) \left[1 + \frac{\Delta_{\text{pg}}^2}{(\omega + \Omega + \xi_{\mathbf{k}+\mathbf{q}}^{\text{pg}})(\omega + \xi_{\mathbf{k}}^{\text{pg}})} \right], \\ \mathbf{\Gamma}(K, Q) &= \boldsymbol{\gamma}(K, Q) - \boldsymbol{\gamma}^{\text{pg}}(K, Q) \frac{\Delta_{\text{pg}}^2}{(\omega + \Omega + \xi_{\mathbf{k}+\mathbf{q}}^{\text{pg}})(\omega + \xi_{\mathbf{k}}^{\text{pg}})}, \end{aligned} \quad (5)$$

where the ‘pg vertex function’ $\gamma^{\text{pg}}(K, Q)$ is chosen such that

$$-i \text{div}_{\mathbf{q}} \gamma^{\text{pg}}(K, Q) = \xi_{\mathbf{k}+\mathbf{q}}^{\text{pg}} - \xi_{\mathbf{k}}^{\text{pg}}. \quad (6)$$

The charge-charge and current-current correlation functions are then given by

$$\begin{aligned} P_{\rho\rho}(Q) &= 2 \sum_K \Gamma_0(K, Q) \gamma_0(K + Q, -Q) G_K G_{K+Q}, \\ \vec{\vec{P}}(Q) &= 2 \sum_K \mathbf{\Gamma}(K, Q) \gamma(K + Q, -Q) G_K G_{K+Q}, \end{aligned} \quad (7)$$

corresponding to the normal phase version of Eqs. (7) and (11) of the main text. The choice of the vertex function in Eq. (5) is non-trivial, but this inference can be checked against both conservation of particles (through the Ward identity, which provides the vertex construction), and less trivially by the different sum-rules.

Superconducting phase

Following standard textbooks, the Ward identity in the superconducting phase is given, using Nambu spinor notation

$$-\Omega \Gamma_0(K, Q) - i \text{div}_{\mathbf{q}} \mathbf{\Gamma}(K, Q) = \tau_3 \mathcal{G}^{-1}(K) - \mathcal{G}^{-1}(K + Q) \tau_3, \quad (8)$$

where τ_3 is the third Pauli matrix (we will also use τ_0 for the identity in Nambu space), and

$$\mathcal{G}(K) = \begin{pmatrix} G(K) & F_{\text{sc}}(K) \\ F_{\text{sc}}(K) & -G(-K) \end{pmatrix}, \quad (9)$$

is the Nambu matrix Green’s function. Note that Γ_μ is now a matrix. For the YRZ model, Eq. (8) becomes

$$-\Omega \Gamma_0(K, Q) - i \text{div}_{\mathbf{q}} \mathbf{\Gamma}(K, Q) = -\Omega \tau_3 + \tau_0 (\xi_{\mathbf{k}+\mathbf{q}} - \xi_{\mathbf{k}}) + \begin{pmatrix} \Delta_{\text{pg}}^2 \left(\frac{1}{\omega + \Omega + \xi_{\mathbf{k}+\mathbf{q}}^{\text{pg}}} - \frac{1}{\omega + \xi_{\mathbf{k}}^{\text{pg}}} \right) & 2\Delta_{\text{sc}} \\ -2\Delta_{\text{sc}} & \Delta_{\text{pg}}^2 \left(\frac{1}{-\omega - \Omega + \xi_{\mathbf{k}+\mathbf{q}}^{\text{pg}}} - \frac{1}{-\omega + \xi_{\mathbf{k}}^{\text{pg}}} \right) \end{pmatrix}. \quad (10)$$

We are interested in the transverse current-current correlation function, which is insensitive to the collective mode physics. This allows us to discard the Δ_{sc} part of the Ward identity (which corresponds to the collective mode singularity of the longitudinal vertex function). We thus infer the transverse vertex function

$$\mathbf{\Gamma}_t(K, Q) = \tau_0 \gamma_t(K, Q) - \gamma_t^{\text{pg}}(K, Q) \begin{pmatrix} \frac{\Delta_{\text{pg}}^2}{(\omega + \Omega + \xi_{\mathbf{k}+\mathbf{q}}^{\text{pg}})(\omega + \xi_{\mathbf{k}}^{\text{pg}})} & 0 \\ 0 & \frac{\Delta_{\text{pg}}^2}{(-\omega - \Omega + \xi_{\mathbf{k}+\mathbf{q}}^{\text{pg}})(-\omega + \xi_{\mathbf{k}}^{\text{pg}})} \end{pmatrix}. \quad (11)$$

The current-current correlation function in the superconducting phase is given by

$$\vec{\vec{P}}(Q) = \sum_K \text{Tr} \left\{ \mathbf{\Gamma}(K, Q) \mathcal{G}(K) \gamma(K + Q, -Q) \mathcal{G}(K + Q) \right\}, \quad (12)$$

where the trace is over the Nambu indices, which gives the transverse current-current correlation function quoted in the main text (Eq.7). We will show next that this choice for $\vec{\vec{P}}(Q)$ is consistent with the transverse sum rule.

TRANSVERSE SUM RULE

The transverse sum-rule is given by $\frac{n_n}{m} = \lim_{\mathbf{q} \rightarrow 0} \int \frac{d\omega}{\pi} \left(-\frac{\text{Im} P_t(i\Omega \rightarrow \omega + i0^+, \mathbf{q})}{\omega} \right)$ (with $P_t(Q)$ the transverse part of $\vec{\vec{P}}(Q)$), where $\vec{\vec{P}}(Q)$ is computed with Matsubara frequencies $i\Omega$. Given the definition of the superfluid density, this sum rule imposes the requirement that $\vec{\vec{P}}(Q)$ discussed above obeys the following Kramers-Kronig relation

$$\lim_{\mathbf{q} \rightarrow 0} \int \frac{d\omega}{\pi} \left(-\frac{\text{Im} P_t(\omega, \mathbf{q})}{\omega} \right) = -P_t(Q = 0). \quad (13)$$

To demonstrate this Kramers-Kronig consistency, we will use the fact that we can rewrite all the Green's functions in $P_t(Q)$ and $P_t(0)$ using spectral functions, and that term by term they give identical contributions.

For example, $G(K)$ can be written as (with $i\omega$ a fermionic Matsubara frequency)

$$G(K) = \sum_i \frac{R_{\mathbf{k}}^i}{i\omega - E_{\mathbf{k}}^i}, \quad (14)$$

where $E_{\mathbf{k}}^i$ are the poles of $G(K)$ and $R_{\mathbf{k}}^i$ the corresponding residues (there are four of them for YRZ). For the other combinations of G , G_0 and F 's, the number of poles is the same, the only difference is in the residues. To simplify the notations, we can rewrite

$$P_t(Q) = \sum_K \sum_a X_a(\mathbf{k} + \mathbf{q}/2) g_a(K) g_a(K + Q), \quad (15)$$

where $a = \{1, 2, 3, 4\}$ indicates the four contributions to P_t , and $X_1(\mathbf{k} + \mathbf{q}/2) = 2 \frac{\partial \xi_{\mathbf{k}+\mathbf{q}/2}}{\partial \mathbf{k}} \frac{\partial \xi_{\mathbf{k}+\mathbf{q}/2}}{\partial \mathbf{k}}$, and $X_2(\mathbf{k} + \mathbf{q}/2) = -2 \frac{\partial \xi_{\mathbf{k}+\mathbf{q}/2}^{\text{pg}}}{\partial \mathbf{k}} \frac{\partial \xi_{\mathbf{k}+\mathbf{q}/2}}{\partial \mathbf{k}}$ and $X_3(\mathbf{k} + \mathbf{q}/2) = 2 \frac{\partial \xi_{\mathbf{k}+\mathbf{q}/2}}{\partial \mathbf{k}} \frac{\partial \xi_{\mathbf{k}+\mathbf{q}/2}^{\text{pg}}}{\partial \mathbf{k}}$ and $X_4(\mathbf{k} + \mathbf{q}/2) = -2 \Lambda^{\text{sc}} \frac{\partial \xi_{\mathbf{k}+\mathbf{q}/2}^{\text{pg}}}{\partial \mathbf{k}} \frac{\partial \xi_{\mathbf{k}+\mathbf{q}/2}}{\partial \mathbf{k}}$. Here $g_1(K) = G_K$, $g_2(K) = F_{\text{pg},K}$, $g_3(K) = F_{\text{sc},K}$, $g_4(K) = \Delta_{\text{pg}}^2 G_0^{\text{pg}}(K) F_{\text{sc},K}$.

We will first compute the left-hand side of Eq. (13) and then show that the right-hand side is consistent with this result.

$$\text{Calculation of } \lim_{\mathbf{q} \rightarrow 0} \int \frac{d\omega}{\pi} \left(-\frac{\text{Im} P_t(\omega, \mathbf{q})}{\omega} \right)$$

It is useful to introduce a relation involving the relevant Matsubara summations

$$h_a(i\Omega) = T \sum_{i\omega} g_a(K) g_a(K + Q) = T \sum_{i\omega} \int_{x,y} \frac{A_{a,\mathbf{k}}(x)}{i\omega - x} \frac{A_{a,\mathbf{k}+\mathbf{q}}(y)}{i\omega + i\Omega - y} = \int_{x,y} \frac{A_{a,\mathbf{k}}(x) A_{a,\mathbf{k}+\mathbf{q}}(y)}{i\Omega + x - y} (f(x) - f(y)), \quad (16)$$

where $f(x)$ is the Fermi distribution and $A_{a,\mathbf{k}}(x)$ is the spectral function of $g_a(K)$, i.e.,

$$g_a(K) = \int \frac{dx}{2\pi} \frac{A_{a,\mathbf{k}}(x)}{i\omega - x}. \quad (17)$$

To prove the sum rule, we need the calculation of

$$\int \frac{d\omega}{\pi} \left(-\frac{\text{Im} h_a(\omega + i0^+)}{\omega} \right) = \int \frac{dx}{2\pi} \frac{dy}{2\pi} A_{a,\mathbf{k}}(x) A_{a,\mathbf{k}+\mathbf{q}}(y) \frac{f(x) - f(y)}{y - x} = H_a(\mathbf{k}, \mathbf{q}). \quad (18)$$

as well as the limit $\mathbf{q} \rightarrow 0$ of $\sum_{\mathbf{k}} X_a(\mathbf{k} + \mathbf{q}/2) H_a(\mathbf{k}, \mathbf{q})$. First, note that the limit $\lim_{\mathbf{q} \rightarrow 0} X_a(\mathbf{k} + \mathbf{q}/2) = X_a(\mathbf{k})$ is well defined. However, one must exercise care with this limit for the product of the two spectral function $A_{a,\mathbf{k}}(x) A_{a,\mathbf{k}+\mathbf{q}}(y)$. The spectral functions are explicitly given by

$$A_{a,\mathbf{k}}(x) = 2\pi \sum_i R_{\mathbf{k}}^{a,i} \delta(x - E_{\mathbf{k}}^{a,i}), \quad (19)$$

and we thus have

$$H_a(\mathbf{k}, \mathbf{q}) = \sum_{i,j} R_{\mathbf{k}}^{a,i} R_{\mathbf{k}+\mathbf{q}}^{a,j} \frac{f(E_{\mathbf{k}}^{a,i}) - f(E_{\mathbf{k}+\mathbf{q}}^{a,j})}{E_{\mathbf{k}+\mathbf{q}}^{a,j} - E_{\mathbf{k}}^{a,i}}. \quad (20)$$

The limit $\mathbf{q} \rightarrow 0$ of $R_{\mathbf{k}+\mathbf{q}}^{a,j}$ is well defined, as is that of $\frac{f(E_{\mathbf{k}}^{a,i}) - f(E_{\mathbf{k}+\mathbf{q}}^{a,j})}{E_{\mathbf{k}+\mathbf{q}}^{a,j} - E_{\mathbf{k}}^{a,i}}$ for $i \neq j$. Thus

$$\lim_{\mathbf{q} \rightarrow 0} H_a(\mathbf{k}, \mathbf{q}) = \sum_{i \neq j} R_{\mathbf{k}}^{a,i} R_{\mathbf{k}}^{a,j} \frac{f(E_{\mathbf{k}}^{a,i}) - f(E_{\mathbf{k}}^{a,j})}{E_{\mathbf{k}}^{a,j} - E_{\mathbf{k}}^{a,i}} - \sum_i (R_{\mathbf{k}}^{a,i})^2 f'(E_{\mathbf{k}}^{a,i}). \quad (21)$$

The first part of the sum-rule thus gives

$$\lim_{\mathbf{q} \rightarrow 0} \int \frac{d\omega}{\pi} \left(-\frac{\text{Im} P_t(\omega, \mathbf{q})}{\omega} \right) = \sum_a \sum_{\mathbf{k}} X_a(\mathbf{k}) \left(\sum_{i \neq j} R_{\mathbf{k}}^{a,i} R_{\mathbf{k}}^{a,j} \frac{f(E_{\mathbf{k}}^{a,i}) - f(E_{\mathbf{k}}^{a,j})}{E_{\mathbf{k}}^{a,j} - E_{\mathbf{k}}^{a,i}} - \sum_i (R_{\mathbf{k}}^{a,i})^2 f'(E_{\mathbf{k}}^{a,i}) \right). \quad (22)$$

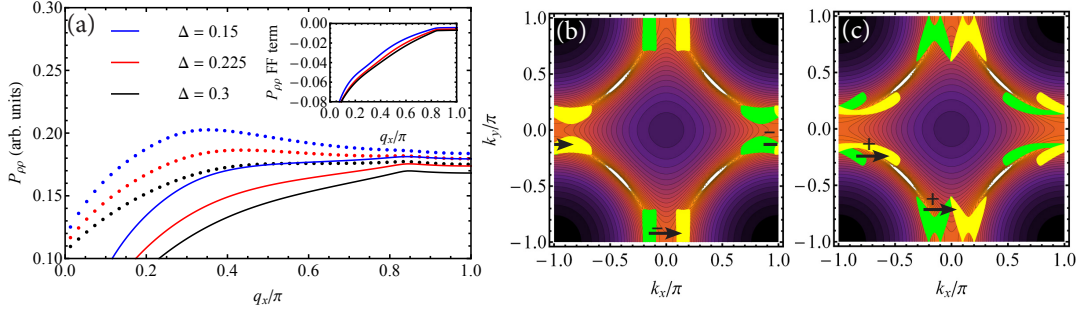


Figure 1: Arc Scenario Results—(a) Normal state $\omega = 0$ charge susceptibility with (solid) and without (dotted) vertex corrections. (b-c) These panels indicate the momentum phase space contributions broken down into (b) the vertex term ($F_{pg}F_{pg}$) and (c) the single fermionic bubble (GG). All parameters are the same as in Figure 1 of the main paper.

Calculation of $P_t(0)$

We start from

$$P_t(0) = \sum_a \sum_K X_a(\mathbf{k}) g_a(K)^2, \quad (23)$$

and we first rewrite the Matsubara sum using the spectral representation

$$T \sum_{i\omega} g_a(K)^2 = T \sum_{i\omega} \int \frac{dx}{2\pi} \frac{dy}{2\pi} \frac{A_{a,\mathbf{k}}(x)}{i\omega - x} \frac{A_{a,\mathbf{k}}(y)}{i\omega - y}. \quad (24)$$

We next integrate over x and y , considering that the Matsubara sum might contain double poles. A straightforward calculation gives

$$\begin{aligned} T \sum_{i\omega} g_a(K)^2 &= T \sum_{i\omega} \sum_{i,j} \int \frac{dx}{2\pi} \frac{dy}{2\pi} \frac{R_{\mathbf{k}}^{a,i} \delta(x - E_{\mathbf{k}}^{a,i})}{i\omega - x} \frac{R_{\mathbf{k}}^{a,j} \delta(y - E_{\mathbf{k}}^{a,j})}{i\omega - y}, \\ &= T \sum_{i\omega} \left(\sum_{i \neq j} \frac{R_{\mathbf{k}}^{a,i} R_{\mathbf{k}}^{a,j}}{(i\omega - E_{\mathbf{k}}^{a,i})(i\omega - E_{\mathbf{k}}^{a,j})} + \sum_i \frac{(R_{\mathbf{k}}^{a,i})^2}{(i\omega - E_{\mathbf{k}}^{a,i})^2} \right), \\ &= \sum_{i \neq j} R_{\mathbf{k}}^{a,i} R_{\mathbf{k}}^{a,j} \frac{f(E_{\mathbf{k}}^{a,i}) - f(E_{\mathbf{k}}^{a,j})}{E_{\mathbf{k}}^{a,i} - E_{\mathbf{k}}^{a,j}} + \sum_i (R_{\mathbf{k}}^{a,i})^2 f'(E_{\mathbf{k}}^{a,i}). \end{aligned} \quad (25)$$

Therefore, we find

$$\begin{aligned} P_t(0) &= \sum_a \sum_{\mathbf{k}} X_a(\mathbf{k}) \left(\sum_{i \neq j} R_{\mathbf{k}}^{a,i} R_{\mathbf{k}}^{a,j} \frac{f(E_{\mathbf{k}}^{a,i}) - f(E_{\mathbf{k}}^{a,j})}{E_{\mathbf{k}}^{a,i} - E_{\mathbf{k}}^{a,j}} + \sum_i (R_{\mathbf{k}}^{a,i})^2 f'(E_{\mathbf{k}}^{a,i}) \right), \\ &= - \lim_{\mathbf{q} \rightarrow 0} \int \frac{d\omega}{\pi} \left(- \frac{\text{Im} P_t(\omega, \mathbf{q})}{\omega} \right), \end{aligned} \quad (26)$$

which shows consistency with the sum rule.

CHARGE ORDERING AND VERTEX FUNCTIONS IN ARCS SCENARIO

The behavior of the charge ordering vertex corrections in the Fermi arcs scenario is presented in Figure 1. This should be compared with the analogous figure in the paper for the Fermi pockets scenario. Here there are no hot spots and therefore no sharp features. Charge ordering in the arcs case (PRB 88, 064516 (2013)) focused on fluctuations at finite ω , where the role of $\omega \neq 0$ and finite γ (both are effectively “pairbreaking”), revealed signatures of the anti-nodal bandstructure.